

WatchDog: Real-time Vehicle Tracking on Geo-distributed Edge Nodes

ZHENG DONG, Wayne State University, USA

YAN LU, New York University, USA

GUANGMO TONG, University of Delaware, USA

YUANCHAO SHU, Microsoft Research Redmond, USA

SHUAI WANG, Southeast University, China

WEISONG SHI, Wayne State University, USA

Vehicle tracking, a core application to smart city video analytics, is becoming more widely deployed than ever before thanks to the increasing number of traffic cameras and recent advances in computer vision and machine learning. Due to the constraints of bandwidth, latency, and privacy concerns, tracking tasks are more preferable to run on edge devices sitting close to the cameras. However, edge devices are provisioned with a fixed amount of computing budget, making them incompetent to adapt to time-varying and imbalanced tracking workloads caused by traffic dynamics. In coping with this challenge, we propose WatchDog, a real-time vehicle tracking system that fully utilizes edge nodes across the road network. WatchDog leverages computer vision tasks with different resource-accuracy trade-offs, and decomposes and schedules tracking tasks judiciously across edge devices based on the current workload to maximize the number of tasks while ensuring a provable response time-bound at each edge device. Extensive evaluations have been conducted using real-world city-wide vehicle trajectory datasets, achieving exceptional tracking performance with a real-time guarantee.

CCS Concepts: • **Computer systems organization** → **Embedded systems**; *Real-time system architecture*.

Additional Key Words and Phrases: Edge Computing, neural networks, real-time system, road network

ACM Reference Format:

Zheng Dong, Yan Lu, Guangmo Tong, Yuanchao Shu, Shuai Wang, and Weisong Shi. 2022. WatchDog: Real-time Vehicle Tracking on Geo-distributed Edge Nodes. *J. ACM* 37, 4, Article 111 (August 2022), 22 pages. <https://doi.org/xxx/xxx>

1 INTRODUCTION

Smart city traffic safety initiatives are springing up across the world as more cities embrace big data and video analytics. A straightforward solution of smart city data analytics is to aggregate data and conduct centralized processing in the cloud. This paradigm, however, has several downsides. First, video data uploading requires a substantial amount of network bandwidth, especially under the increasing number of high resolution cameras. Second, cloud-based processing

This work was supported in part by the U.S. National Science Foundation under Grants CNS-2140346, CNS-2103604 and in part by a start-up Grant from Wayne State University.

Authors' addresses: Zheng Dong, dong@wayne.edu, Wayne State University, 42 W Warren Ave, Detroit, Michigan, USA, 48202 ; Yan Lu, jasonengineer@hotmail.com, New York University, New York, New York, USA; Guangmo Tong, amotong@udel.edu, University of Delaware, Newark, USA; Yuanchao Shu, yuanchao.shu@microsoft.com, Microsoft Research Redmond, Redmond, USA; Shuai Wang, shuaiwang@seu.edu.cn, Southeast University, Nanjing City, China; Weisong Shi, weisong@wayne.edu, Wayne State University, 42 W Warren Ave, Detroit, Michigan, USA, 48202.

Permission to make digital or hard copies of all or part of this work for personal or classroom use is granted without fee provided that copies are not made or distributed for profit or commercial advantage and that copies bear this notice and the full citation on the first page. Copyrights for components of this work owned by others than ACM must be honored. Abstracting with credit is permitted. To copy otherwise, or republish, to post on servers or to redistribute to lists, requires prior specific permission and/or a fee. Request permissions from permissions@acm.org.

© 2022 Association for Computing Machinery.

Manuscript submitted to ACM

Manuscript submitted to ACM

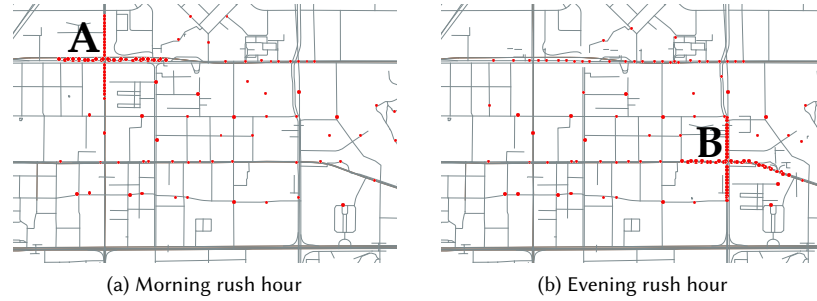


Fig. 1. Snapshots of traffics during different rush hours in the city of Shenzhen, China. Red dots denote vehicles traveling in this area.

adds up latency, which could be prohibitively high for smart city applications such as amber alerts or traffic light control. Third, privacy becomes more of an issue when public information is uploaded and stored in the cloud.

In coping with such challenges, an increasing number of smart edge devices, such as Azure Stack Edge [1], Argonne Waggle and Intel Fog Reference, are being developed and deployed in cities around the world. Such smart edge devices enable fast local computation and have benefited security surveillance systems such as induction coil system [32], traffic surveillance system [6] and the suspicious object monitoring system [23]. The shift in computing paradigm from the cloud to the edge has also necessitated the adoption of new programming models, algorithms, and analytics methods to fully exploit the computing capacity of multi-core chips deployed on the edge. Edge node manufacturers and application developers are starting to discover ways to multiplex tasks and share resources across nodes in an edge cluster [10, 21, 25]. These advanced edge computing approaches provide new possibilities for designing real-time video analytics systems, which leverage machine learning for tasks like object detection and re-identification. In this paper, we focus on multi-camera vehicle tracking, a core application of the smart city video analytics system, and study how to leverage geo-distributed edge nodes to build a reliable real-time tracking system.

Motivation: Edge nodes are provisioned with a fixed compute budget. For instance, Azure Stack Edge [1] node has 2×10 core CPUs and 128 GB memory. Even though they are beefy enough to handle computational demands for real-time data processing in most cases, in some corner cases, when the number of vehicles appearing in the monitored areas is too large, the corresponding data processing may not be able to complete in time, leading to a fatal failure for the whole system. Fig. 1 shows the snapshots of traffic conditions during different rush hours in Shenzhen. Suppose that a real-time tracking system is implemented on the edge node at each intersection to track hit-and-run vehicles (Assuming that the hit-and-run accident is detected and reported instantly in smart cities and the tracking system can obtain the location of the accident and the information of the VoI immediately). As seen in Fig. 1(a), at most of the intersections, only one or two vehicles appear in the monitored areas and hence the tracking system can run complex vision algorithms on each of the vehicles and identify Vehicle-of-Interest (VoI) easily. However, during morning rush hours, the number of vehicles at intersection A grows substantially. Thus, identifying VoI from all vehicles traveling through intersection A in real-time requires far more computing resources, which may exceed the computing capacity of the edge node. If the VoI cannot be identified at intersection A, the tracking system will lose the VoI. Similar patterns are observed at intersection B, where the corresponding edge node falls short during evening rush hours. On the other hand, computing budget provision on all edge nodes based on the worst case scenario is also a non-starter due to the high upfront investment and low resource utilization. In light of the tension between traffic variations and the fixed amount of edge computing resources, this paper aims to answer a simple question: can we collaboratively utilize the

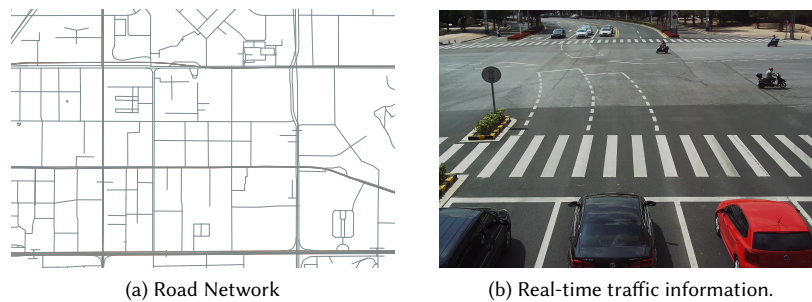


Fig. 2. A road network and surveillance video at an intersection.

existing geo-distributed edge nodes deployed in the city to provide a reliable tracking system without “tracking loss” at crowded intersections?

Inspired by the idea of collaborative tracking (i.e., the tracking task will be decomposed and scheduled judiciously across the distributed edge nodes based on real-time traffic conditions), in this paper, we propose the design of an intelligent real-time tracking system in smart cities, named WatchDog, to track vehicles across intersections. There are two major components in WatchDog: *a real-time admission control policy* and *a novel dynamic Vehicle - ReID framework*. WatchDog models video analytics executed on an edge node to ReID the VoI as a real-time system: each real-time task corresponds to a vehicle re-identification module performed on a detected vehicle. The execution time of a real-time task depends on the vehicle re-identification module chosen from the dynamic Vehicle - ReID framework, and whether or not each real-time task can complete in real-time is verified by the admission control policy. The longer the tasks execute, the less chance the real-time task system has to pass the admission control. By combining the real-time admission control policy with the dynamic Vehicle - ReID framework together, WatchDog builds a reliable tracking system without “tracking loss” at crowded intersections.

Example: Suppose a Mercedes silver GLB SUV (which is the VoI) is involved in a hit-and-run accident. When it enters a crowded intersection, the computation capacity on the edge node is not enough to perform the most fine-grained re-identification method to check each vehicle and identify VoI. Then the Vehicle - ReID module is downgraded to a coarse but more lightweight method to identify the vehicles’ colors and models, which is determined by the admission control policy. The tracking system detects all silver SUVs at the crowded intersection, which are traveling to different neighboring intersections. The tracking system informs the edge nodes to ReID the VoI at corresponding intersections. When the silver SUVs enter the intersections where the traffic is light, the VoI will be identified through advanced matching methods and the other silver SUVs will be eliminated. Following this method, the “tracking loss” issue is solved. Our specific contributions are listed as follows:

- We propose a simple yet effective real-time system for tracking hit-and-run vehicles in smart cities, which for the first time enables us to collaboratively utilize the distributed edge resources in the road network to enhance the performance of the whole tracking system.
- To the best of our knowledge, this is the first in-depth work to investigate the combined effect of video processing latency and real-time traffic conditions, which are not discussed in the existing solutions. A real-time admission control policy and a novel dynamic Vehicle - ReID framework are proposed to resolve the “tracking loss” issue.

- We have extensively evaluated WatchDog using our accessible real-world vehicle system-wide datasets. Experimental results show that WatchDog can achieve exceptional tracking performance in real-time without “tracking loss”.

2 RELATED WORK

Not surprisingly, a large number of works have been conducted to understand intelligent urban edge computing with public security surveillance systems, including intelligent transportation system realization [38, 53, 59], traffic flow analytics [3, 34, 48] and driving routes optimization [17, 32, 46]. However, in our work, we consider building a real-time vehicle tracking system, which fully utilizes edge nodes across the road network. Since the topic is novel, similar studies on real-time vehicle tracking with video surveillance cameras are few, but include [7, 36, 54].

Especially, [54] designs and implements a self-adapting hit-and-run vehicle tracking algorithm with distributed sparse video surveillance cameras and mobile taxicabs, leveraging time-varying characteristics of road traffic flow patterns. By mining the massive trajectory dataset of taxicabs and a video dataset of surveillance cameras, the travel time-cost of a road segment during a specific time period is modeled using a Logarithmic Normal Distribution, which calculates the time-cost of an urban trip during a specific time period with a Log Skew Normal Distribution approximately. This work trains the model offline and does not consider resource management while tracking a VoI in real-time. With the emergence of vehicle-mounted GPS navigation systems and vehicular networks, a collection of series of GPS coordinates became available for vehicle tracking. Based on the GPS records, [36] proposes a novel global map-matching algorithm utilizing the spatial geometric/topological structures of the road network as well as the temporal/speed constraints of the trajectories. The basic assumption that true paths of vehicles tend to be direct rather than roundabout is used to enhance the accuracy of computing actual vehicle trajectories. But for VoIs, if they choose abnormal paths to avoid the tracking system, it will increase the difficulty of trajectory recovery. [7] develops an efficient machine learning-based method for vehicle detection and motion analysis in the low-altitude airborne platform. This work has not considered cooperative computing with multiple video cameras, since the deployments of fixed video cameras are still distributed, sparse and cannot support the seamless monitoring of the VoI in nature.

Specific to the problem investigated in this paper, existing studies on recovering detailed trajectories of vehicles with GPS coordinates are designed for normal vehicles, which cannot be used to track VoIs. Moreover, in practice, we cannot even obtain any GPS information of VoIs and videos from the taxicabs, and the information from the public security surveillance system and the computing capacity on the edge nodes are the only resources we can leverage.

3 BASIC SETUP AND SYSTEM MODEL

3.1 Basic Setup

Given the road network in the urban area of a smart city, this paper aims to find a method to track the VoI (e.g., hit-and-run vehicles) by combining the information from fixed video surveillance cameras and the road network, thereby helping the tracking system track the VoI in real-time using minimum edge resources. The basic settings of this paper are outlined as follows:

- **Road Network:** Fig. 2 shows a road network in the urban area of Shenzhen with intersections and road segments. Surveillance cameras are deployed at the intersections to capture real-time traffic information.
- **Edge nodes:** Consistent with existing deployments, our focus is on “edge” computation of video analytics. In our setup, one edge node is deployed at each intersection, which consists of a surveillance camera and a

209 computing platform. A video captured by the camera is streamed to this edge box and the pipeline modules
 210 including object detection and re-identification algorithms are run on this edge node.

- 211 • **Cloud:** Each edge node only captures and processes local information at the intersections. In order to get a
 212 global view of the entire monitored area, the cloud collects the processing results from all the edge nodes. Hence
 213 the tracking system includes both edge nodes and the cloud.
 214
 215

216 3.2 System Model

217 In this subsection, we define the road network and vehicle trajectory used in our system model.

219 **Definition 1. (Road Network)** The road network consists of intersections and road segments between intersections,
 220 which can be modeled as a graph $G(V, E)$ where the vertex set V denotes all intersections and the edge set E corresponds
 221 to all road segments. Intersection $I_i \in V$ and $e_{i,j} \in E$ if there exists a road segment from intersection I_i to intersection I_j .

223 **Definition 2. (Vehicle Trajectory)** For an arbitrary vehicle, which travels in the road network, its trajectory in one
 224 specific day d can be formulated by $T = \{I_o(t_1, t_2), I_{o+1}(t_3, t_4), \dots, I_e(t_x, t_{x+1})\}$, which means this vehicle is firstly
 225 detected at intersection I_o , then ends at intersection I_e . For one element $I_y(t_k, t_{k+1})$ in this trajectory, t_k is the time
 226 instant that the vehicle enters intersection I_y and time instant t_{k+1} corresponds to the time it leaves this intersection.
 227
 228

229 **Definition 3. (The Tracking System)** The tracking system includes both the edge nodes and the cloud. The object
 230 recognition algorithms are implemented on the edge nodes. At the very beginning, when a hit-and-run accident is
 231 reported to the tracking system, the first edge node is activated instantly according to the location of the accident.
 232 During the *active period* of the edge node, it identifies the VoI and the next intersection on the VoI's trajectory based on
 233 real-time video analytics. The analysis results are uploaded to the cloud to activate the edge node deployed at the next
 234 intersection and stop the previous one. From then on, the next activated edge node and its active period depend on the
 235 analysis results performed at the previous intersection and the historical traffic information (which will be discussed in
 236 section 7). The communication between edge nodes is enabled through the cloud.
 237
 238

239 Intuitively, if the tracking system knows when the VoI will arrive at which intersections in advance, the corresponding
 240 edge nodes can be activated during specific periods to track the VoI in real-time. However, in practice, the implementation
 241 of real-time tracking is very challenging.
 242
 243

244 3.3 Tracking Loss Issue

245 Fig. 3 shows an example of a road network consisting of 16 intersections. Suppose a hit-and-run vehicle has a trajectory
 246 of $T = \{I_1(t_1, t_2), I_2(t_3, t_4), I_6(t_5, t_6), I_7(t_7, t_8), I_{11}(t_9, t_{10}), I_{12}(t_{11}, t_{12})\}$ in the monitored area. Then, the edge nodes
 247 deployed at $I_1, I_2, I_6, I_7, I_{11}, I_{12}$ are involved in tracking the VoI. If we ignore the time periods taken by the vehicle at the
 248 intersections, the trajectory T can be considered as a path in the road network, i.e., $I_1 \rightarrow I_2 \rightarrow I_6 \rightarrow I_7 \rightarrow I_{11} \rightarrow I_{12}$. In
 249 this paper, the tracking system aims to track the VoI in real-time: if the VoI enters I_i at time instant t_p , then
 250
 251

- 252 • the edge node at I_i must be activated before t_p . Otherwise, the VoI may not be captured by the camera and get
 253 lost at I_i .
- 254 • the VoI and the next intersection I_j on the VoI's trajectory must be identified before the time instant t_q when
 255 the VoI enters I_j . Otherwise, the tracking system cannot activate the edge node at I_j before t_q .
 256
 257

258 **Example 1.** For the example in Fig. 3, a Mercedes silver GLB SUV (the VoI) is reported to be involved in a hit-and-run
 259 accident at intersection I_1 at time instant t_1 and it arrives at I_2 at t_3 . The edge node at I_1 is activated at t_1 : the camera
 260

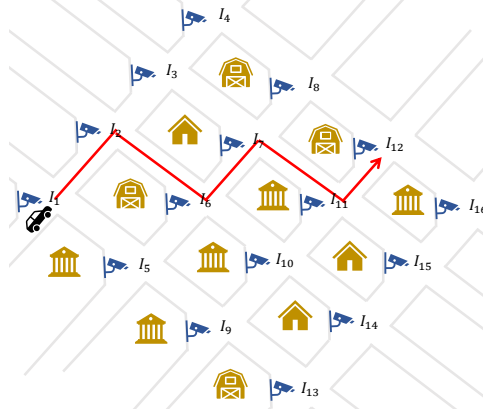


Fig. 3. An example of vehicle real-time tracking

captures videos from I_1 and the videos are processed frame-by-frame to identify the VoI and the next intersection on the VoI's trajectory. The processing results must be obtained and sent to the cloud before t_3 . Then, the tracking system can activate the edge node at I_2 before t_3 ; otherwise, the VoI may already depart from I_2 before the edge node starts tracking.

Note that the next intersection on the VoI's trajectory can be easily determined by the VoI's position and the road network based on a series of video frame processing.

If the tracking system tracks the VoI in real-time successfully, the VoI will be located at either an intersection or a road segment between two intersections at any specific time instant when it travels in the monitored area. The tracking problem becomes rather trivial to resolve if only a few vehicles travel in the smart city. It means that whenever the VoI appears at an intersection, it will be recognized by the object identification algorithms instantly due to sufficient computing resources on the edge node. However, the practical scenario is always not the case.

Example 2. In Fig. 3, the VoI arrives at intersection I_2 at time instant t_3 and travels to I_6 . Assume that I_2 is a crowded intersection. In this case, it takes a very long time to identify the VoI from dozens of cars traveling through the intersection. The edge node at I_2 may fail to complete the video analytics when the VoI arrives at I_6 at t_5 . Then, the tracking system does not know which edge nodes should be activated afterward to carry on the tracking task and the VoI is lost.

Identified issue. The computing capacity of an edge node depends on the computing platform used to implement it, which is determined by the hardware manufacturer. For example, an Azure Data Box Edge [1] node is equipped with 2×10 core CPUs for data processing. Thus, at the crowded intersections, the tracking system cannot identify the VoI in real-time due to the limited computing capacity of the edge node and the "tracking loss" occurs.

Key idea of our proposed method. To resolve this "tracking loss" issue, we seek to develop a smart tracking method to make up for the limited computing capacity of a single edge node. At a crowded intersection, since the full-fledged object identification algorithm needs an unaffordable amount of time to precisely find the VoI, the tracking system can use a "coarse" object identification algorithm to save time. Multiple suspected VoIs may be identified by the "coarse" algorithm and travel to different intersections. The tracking system can track all the suspected VoIs simultaneously by utilizing the edge nodes at different intersections and identifying the VoI at the uncrowded intersections. Intuitively,

313 this idea is feasible, because we find that almost 95% of the intersections in a smart city are uncrowded intersections
314 (See the statistics in Sec. 9.1.2).

315 In order to implement the real-time tracking system, first we propose a dynamic Vehicle Re-Identification (Re-ID)
316 framework to realize the Re-ID algorithm at different granularity levels. Then we introduce a real-time admission
317 control module on each edge node to decide which Re-ID algorithm will be performed to identify the VoI according to
318 the number of vehicles detected at the corresponding intersection. Finally, we will discuss how to obtain the active
319 period for each edge node involved in a hit-and-run tracking event and how the proposed tracking system, named
320 *WatchDog*, works to track the VoI in real-time.
321
322

324 4 VISION-BASED VEHICLE TRACKING

326 Tracking in WatchDog relies on computer vision-based machine learning algorithms. Query input is a target vehicle
327 (e.g., from an accident report) with information such as make, model, color, and plate number. Once WatchDog receives
328 a tracking query, the corresponding edge node starts running a video analytics pipeline to analyze traffic videos in
329 real-time. At a high level, the processing pipeline of each frame consists of two modules: vehicle detection and vehicle
330 re-identification.
331

333 4.1 Vehicle Detection

335 For each video frame, vehicle detection targets to find all vehicles and assign a class to each one of them. Unlike
336 classification networks, traditional vehicle detection networks [15, 27, 31, 47] have three components: a CNN-based
337 feature extractor, Region Proposal Network (RPN) and a classifier. They usually use a pre-trained classification network
338 (e.g., ResNet) as a feature extractor to a generate feature map of an input image. After that, they utilize RPN [15] to
339 generate all candidate bounding boxes of vehicles, and finally assign labels for each bounding box. As those detectors
340 extract all vehicles first and classify each bounding box later, they are called two-stage vehicle detectors. Although
341 two-stage vehicle detectors achieve superior performance on many public benchmarks [2, 4, 39], the speed suffers. To
342 trade-off performance and latency, researchers seek to design efficient vehicle detectors [29, 30, 51, 55] which use one
343 CNN network to solve localization and classification simultaneously. Albeit marginal performance drop, one-stage
344 detectors largely reduce latency, and hence have been widely implemented on today's edge nodes for real-time tracking
345 systems.
346
347
348
349

350 4.2 Vehicle Re-identification

351 Vehicle re-identification (V-ReID) determines whether two bounding boxes belong to the same vehicle. The most popular
352 deep learning approach for V-ReID is to build a CNN-based feature extractor and differentiate bounding boxes based on
353 the similarity (e.g., cosine distance) between discriminative feature vectors. Unlike person re-identification (P-ReID),
354 V-ReID [22, 24, 43, 50, 57] often uses many CNN-based networks to extract different features (e.g., global features, region
355 features, key point features) and concatenate them for a reliable comparison. For example, researchers often set features
356 of a vehicle's shape as a general feature and window screen as a region feature. As a result, V-ReID models are often
357 very large and the end-to-end compute process is prohibitively costly, making them not amenable to real-time tasks.
358 For example, V-ReID each one of a large set of vehicle bounding boxes during the rush hours could end up causing
359 "tracking loss" issue. Thus, a V-ReID method that can dynamically trade-off accuracy with inference time in real-time is
360 desired. To this end, in what follows we propose a dynamic V-ReID framework called D-V-ReID.
361
362
363
364

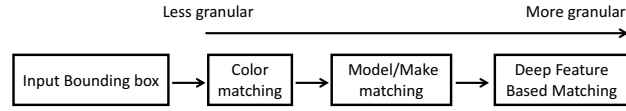


Fig. 4. Layered modules.

4.3 D-V-ReID Pipeline

D-V-ReID adopts the idea of divisive clustering where V-ReID on each frame follows a multi-layer framework where upper layers correspond to coarse but efficient classifications and lower layers are in charge of powerful but complex detection. While we need to slightly modify the existing learning algorithm for the purpose of real-time tracking, we do not intend to propose any new learning algorithm in this paper but focus on building a flexible V-ReID pipeline. The cascaded pipeline we propose includes: color matching, model and make matching, and the full-fledged deep feature-based re-identification.

4.3.1 Color Matching. As a basic filter, color matching measures similarity between bounding boxes by color distribution in spaces such as RGB or HSI [16]. Given RGB or HSI features, we use K-Nearest Neighbors (KNN) [12] to decide the similarity of two images. A car is classified by a majority vote of its neighbors, with the car being assigned to the class which is most common amongst its k nearest neighbors. The complexity of the inference process in this step is linear to the input frame size, and it can be further reduced by frame down-sizing, which provides a trade-off between matching quality and inference time where the inference time can be made arbitrarily small. As the most coarse V-ReID step, a matching confirm result does not provide much confidence that the target vehicle is detected because different vehicles may have similar color, but a matching reject serves as strong evidence for the fact that the target vehicle is not in the current frame.

4.3.2 Model and Make Matching. Our second layer aims to detect if the vehicle in the bounding box has the same model and make as the target vehicle. Model and make of a vehicle are more distinctive, and such information is commonly used for vehicle identification in security systems such as amber alerts. Traditional matching algorithms use Scale Invariant Feature Transform (SIFT) [37], SURF [20] and HOG [40] feature extraction techniques to extract models' features. Based on these features, Support Vector Machine [41, 44] and Random Forest [52] can matching two cars accurately. But these methods assume that the input image has the whole shape of the vehicle. In practical environments, many cars are occluded by other objects. To resolve this issue, many works [13, 28] seek to use deep learning approaches to generate discriminative features because of the ability to extract features automatically. Unlike general image classification or object detection, model and make matching on vehicle is done by training a light convolutional neural network (ResNet50, MobileNet, ShuffleNet, EfficientNet [19, 45, 49, 60]). For instance, we could adopt a subset of ResNet for such a purpose. The goal of model and make matching in our framework is still to provide a fairly accurate V-ReID method with moderate inference overhead.

4.3.3 Full-fledged V-ReID. Deep feature-based V-ReID algorithm serves as the final layer in D-V-ReID. In light of ensemble learning [9], start-of-the-art V-ReID methods [5, 14, 42, 50, 61] are designed with a set of convolutional neural networks, and these neural networks are responsible for different feature extractions. To further improve ReID accuracy, researchers assign unique loss functions [57] to different feature extractors and train them independently. After pre-training, a unified loss function is utilized to train all feature extractors together. This step is also called

Table 1. Cost of deep feature extractors (global, region and key-point features).

	Global	Region	Key-point
Flops	341.5M	7868.4M	11392.M
Inference Time	41.1ms	96.7ms	172.3ms
CPU Usage	2.4%	9.8%	15.0%

Table 2. Cost of different modules (color matching, model matching and full-fledged V-ReID).

	Color	Model	Full-fledged V-ReID
Flops	/	341.5M	19602.3M
Inference Time	0.5ms	40.6ms	310.1ms
CPU Usage	0.3%	2.2%	27.3%

multi-task learning [14, 50, 56, 58]. In particular, these methods always classify features as global, region and key-point features. The global feature is used to describe the overall appearance of the vehicle, which is the linear transformation of the pooling feature of the last convolution module in global feature extractor. Due to the limited discriminative ability of global features, many researchers seek to use multiple granularities network [18] to extract features from the multiple semantic parts of vehicles. Inspired by [61], scientists use another CNN network to predict several key points sit on key parts of the vehicle (e.g., the vehicle license plate), and then extract features around those key parts with the assistance of a heat-map generated from key point network. In our design, we combine features from color matching and model/make matching, and set it as the global feature. The reason for doing so is to provide early exit and reuse computation from previous matchings.

4.4 D-V-ReID framework.

D-V-ReID framework is built upon three V-ReID algorithms with different granularity levels, which is illustrated in Fig. 4. As discussed above, we set K-Nearest Neighbors classifier [12] as our color filter and the architecture of model matching to MobileNetV2 [45]. In terms of the full-blown V-ReID, we adopt the best method [57] in AI City Challenge 2019. They utilized three different convolution neural networks to extract features from the same vehicle and concatenate them as the final feature. As discussed in Section 4.3.3, we combine features from color matching and model/make matching as the global feature. To see the computation cost of region and key-point feature extractors, we set their architectures to ResNet101 [19] and SE-ResNet152 [26], respectively. After re-scaling each bounding box to $224 * 224$, we report floating point operations per second (flops), inference time and cpu usage on one bounding box of different feature extractors from deep feature based matching in Table 1 and different modules in Table 2. The test environment is AMD Ryzen 7 3700x (CPU) with 4G memory. Because K-Nearest Neighbors classifier is not a deep neural network, we don't record the flops for it.

According to the real-time requirements of the tracking system, it could select the V-ReID modules with a proper complexity to identify the VoI at specific intersections. Intuitively, in order to guarantee that the V-ReID module can complete in real-time, a less granular module will be triggered if a large number of vehicles appear at a crowded intersection. On the contrary, if the intersection is uncrowded, a more granular module will be performed to identify VoI. Note that under our proposed D-V-ReID framework, if a more granular module is selected, all the less granular modules are executed implicitly. It is evident that the granularity selection depends on the number of vehicles captured

on each video frame, the inference time of different V-ReID modules and the computing capacity of the edge node. In next section, we introduce a real-time admission control method, which is implemented on each edge node to select proper V-ReID modules for the tracking system in real-time.

5 REAL-TIME ADMISSION CONTROL

Before discussing the details of our design, we introduce some preliminary results on real-time admission control, which determines the granularity level of the V-ReID modules selected to identify the VoI.

5.1 Real-Time Task Scheduling Framework

In this section, we will introduce a classic soft real-time schedulability test, which can be used to calculate the completion time bounds for real-time tasks scheduled in the real-time system. Based on the completion time-bound of each real-time task, we can perform admission control on each edge node.

5.1.1 Real-time Task Model. At an arbitrary intersection I_x , the surveillance camera captures frames from the intersection periodically and the *period*, denoted by p , depends on the camera's frequency. For example, if the camera captures 24 frames every second, we would say the video is 24 fps and its period is $\frac{1}{24}$ s. Usually, one or more vehicles may be detected on each frame. The V-ReID machine learning algorithm is performed on all the detected vehicles to identify the VoI and each identification process corresponds to a *real-time machine learning task*. Let e_i denote the *processing time* of task τ_i performed on vehicle i . Tabel 2 gives the processing time for different V-ReID modules. Let e^c, e^m, e^d denote the processing time for color matching module, model/make a matching module, and Deep Feature-Based Matching module, respectively. Under our proposed D-V-ReID pipeline framework, if a more granular module is selected, all the less granular modules has already been selected implicitly. Thus, e_i has three different options under the D-V-ReID framework: $e_i^1 = e^c, e_i^2 = e_i^1 + e^m, e_i^3 = e_i^2 + e^d$. As we discussed in Sec. 7.1, in order to avoid "tracking loss", the VoI must be identified before it arrives at the next intersection (it is illustrated by Example 2).

Definition 4. Let $t_{x,y}$ denote the traveling time of the VoI between two neighbouring intersections (i.e., I_x and I_y). I_x may have multiple neighbouring intersections and we define the shortest $t_{x,y}$, denoted by D_x , as the *relative deadline* of the real-time tasks from the edge node deployed at I_x .

Based on the above discussion, we use the periodic hard real-time task model to describe the execution behaviors of real-time workloads in the tracking system on an edge node deployed at I_x . We consider the problem of scheduling n periodic real-time tasks on M processors. That means n vehicles are detected from each image and the edge node has M processors (note that we use "processor" to denote the minimum schedulable processing unit). A task τ_i is characterized by two parameters - a processing requirement e_i and a period p with the interpretation that the task generates a job (i.e., the camera captures a frame) in every p time units and each such job $\tau_{i,j}$ has a processing requirement of e_i execution units which should be met by a deadline $d_{i,j}$. Let $r_{i,j}$ denote the generation time of $\tau_{i,j}$, then $d_{i,j} = r_{i,j} + D_x$. We further let u_i denote the utilization of τ_i , where $u_i = \frac{e_i}{p}$, and the utilization of the task system τ is defined as $U_{sum} = \sum_{i=1}^n u_i$. Successive jobs of the same task are required to execute in sequence. We require $u_i \leq 1$, and $U_{sum} \leq M$; otherwise, deadlines will be missed.

5.1.2 Real-time Scheduling Algorithm. If the number of tasks is no greater than the number of processors, each identification task can be executed on a dedicated processor. In this case, the computing capacity on the edge node is sufficient to execute the real-time tasks and the "tracking loss" issue will not happen. However, when the traffic is

heavy, the number of vehicles (corresponding to the real-time tasks) detected at the intersection may be much larger than the number of processors on the edge node. The real-time tasks will compete for the limited computing resources on the edge node and have inferences with each other, which may give rise to a huge delay for frame processing and lead to deadline miss. In this case, a scheduling algorithm is needed to allocate processor time to tasks, i.e., determines the execution-time intervals and processors for each job while taking any restrictions, such as on concurrency, into account. In real-time systems, processor-allocation strategies are driven by the need to meet timing constraints and in our real-time tracking system, we apply the First-in First-Out (FIFO) policy to schedule the real-time tasks: processors execute jobs in the exact order of job arrival.

5.1.3 Completion Time Analysis. A given set of real-time tasks is said to be schedulable on a given system of processors if the tasks can be scheduled on these processors in such a manner that all jobs of all the tasks always complete by their deadlines. Physically, if all the tasks can complete by their deadlines, the “tracking loss” will not happen. The schedulability can be verified by using standard schedulability analysis (Theorem 1) for calculating the completion times of real-time tasks.

THEOREM 1. *Considering that a real-time task system τ of n periodic tasks are scheduled on M processors under FIFO scheduling policy, the completion time bound for a task τ_i is*

$$R_i = p + e_i + \frac{\sum_{\tau_k \in E(\tau, M-1)} e_k - e_i}{M - \sum_{\tau_j \in U(\tau, M-1)} u_j} \quad (1)$$

where $E(\tau, M-1)$ denotes the set of at most $(M-1)$ tasks with the highest execution costs from τ and $U(\tau, M-1)$ denotes the set of at most $(M-1)$ tasks of highest utilization from the task set τ [33].

The proof of Theorem 1 is given in [33] and the same result can be derived from [11], because the periodic task model is a special case of the stochastic task model discussed in [11]. In light of the real-time task model and the completion time analysis, a formal definition of “tracking loss” is that if the completion time bounds of the real-time tracking tasks exceed their deadlines, the VoI is lost at some intersections.

5.1.4 Real-time Admission Control. Intuitively, if we can guarantee that the completion time bound R_i for each task τ_i can be no greater than its deadline D_x , the “tracking loss” cannot happen. According to Theorem 1, since p and M are fixed values when the hardware of the edge node is given, the completion time bound R_i of τ_i only depends on the execution times of the machine learning tasks and the number of vehicles detected at the intersection. Therefore, we introduce the following programming to select proper V-ReID modules for the tracking system in real-time.

$$\begin{aligned} & \text{maximize} && \sum_{i=1}^n e_i \\ & \text{subject to} && R_i = p + e_i + \frac{\sum_{\tau_k \in E(\tau, M-1)} e_k - e_i}{M - \sum_{\tau_j \in U(\tau, M-1)} u_j} \leq D_x, \\ & && e_i \in \{e_i^j, e_i^{j+1}\}, \quad j = 1, 2 \end{aligned} \quad (2)$$

where e_i denotes the execution time of task i in the j^{th} iteration. According to Tabel 2, the processing time of color matching module is 0.5 ms. We assume that the edge node has enough computing capacity to perform color matching module on all detected vehicles even at the most crowded intersection. Thus, in the first iteration, our objective is to maximize the number of tasks which will perform the model/make matching module. If all the tasks can meet the deadline, then in the second iteration, we aim to maximize the number of tasks which will perform the deep feature matching module. R_i is the response time of task i , which is defined in Theorem 1, and D_x is the relative deadline

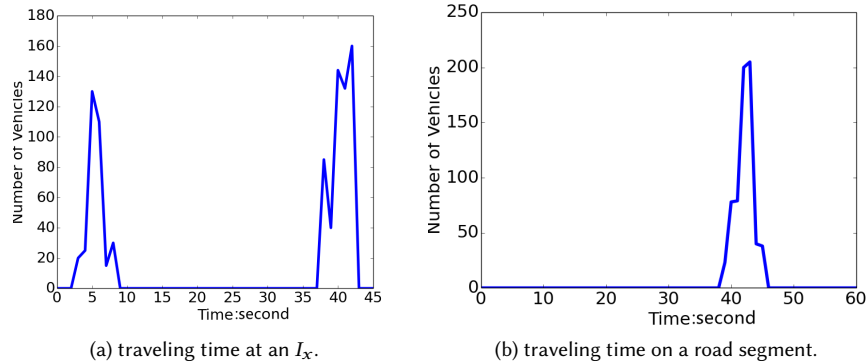


Fig. 5. traveling time measurement at different locations. The x-axis denotes the traveling time and y-axis denotes the number of vehicles traveling through this location.

of every real-time task from I_x , which is defined by Def. 7. We require that each task must complete by its deadline. Since we do not have preferences for the tasks which will perform in the j^{th} iteration, the time complexity for this programming is $O(n)$ to achieve the optimal solution.

6 ACTIVE PERIODS OF EDGE NODES

In order to track the VoI in real-time, the tracking system should be able to know when the VoI will arrive at which intersections in advance, then the corresponding edge nodes can be activated before the VoI's arrival time and identify the VoI when it appears. In other words, the active period of an involved edge node should cover the time interval when the VoI travels through the corresponding intersection.

If all the intersections are uncrowded, this problem is trivial. For the example in Fig. 3, when the hit-and-run accident is reported, the edge node at intersection I_2 is activated to perform the most granular machine learning algorithm on all detected vehicles and the VoI is identified at time instant t_1 . Based on the real-time video analytics, the tracking system finds that the VoI departs from I_2 and travels to I_3 at time instant t_2 . Then, the tracking system activates the edge node at I_3 instantly and at the same time stops the edge node at I_2 . If the tracking system repeats the same operation on all involved edge nodes, the active period for each edge node can be obtained in real-time.

However, when the VoI enters a crowded intersection, the problem becomes challenging. Assume that intersection I_3 is a crowded intersection in Fig. 3 and the VoI (a Mercedes silver GLB SUV) is traveling from I_2 to I_3 . The admission control module selects the color matching module to track all the silver vehicles traveling through I_3 based on the number of vehicles detected in the video frames. Multiple silver vehicles may appear in I_3 , but the tracking system cannot confirm that whether or not the VoI has arrived at I_3 . Because the traveling time on the road segment between I_2 and I_3 is different for different vehicles. Fig. 5 shows the traveling time measurement at different locations. On a road segment, the traveling time of vehicles varies within a range from 30 seconds to 50 seconds (Fig. 5.b). Thus, at a crowded intersection, in order to guarantee that VoI is included in the tracked vehicles (in the example, VoI is one of the tracked silver vehicles), the active period for the edge node is calculated based on historical traffic information.

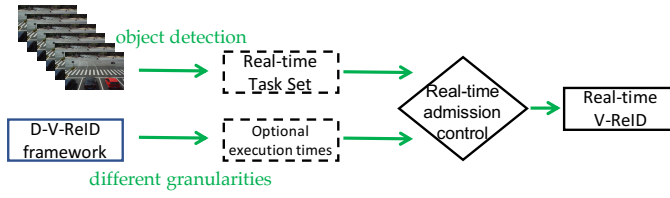


Fig. 6. The architecture of WatchDog implemented on the edge node.

Definition 5. Let t_x denote the traveling time taken by the VoI at intersection I_x , then $t_x^l \leq t_x \leq t_x^u$, where t_x^l is the lowest value among all the vehicles' traveling time at I_x and t_x^u is the largest value. Both values can be obtained from historical traffic information (For example, Fig. 5.a).

Definition 6. Suppose I_x and I_y are neighbouring intersections. Let $t_{x,y}$ denote the traveling time taken by the VoI at road segment $e_{x,y}$, then $t_{x,y}^l \leq t_{x,y} \leq t_{x,y}^u$, where $t_{x,y}^l$ is the lowest value among all the vehicles' traveling time at $e_{x,y}$ and $t_{x,y}^u$ is the largest value. Both values can be obtained from historical traffic information (For example, Fig. 5.b).

Definition 7. Note that according to Definition 4 and Definition 6, I_x may have multiple neighbour intersections and we use the shortest $t_i^{x,y}$ as the *relative deadline* D_x of the real-time tasks from the edge node deployed at I_x .

Based on Definition 5, Definition 6 and Definition 7, we can calculate the active period $[t_x^s, t_x^e]$ for an involved edge node at intersection I_x .

- **Case 1:** If the previous intersection I_p on the VoI's trajectory is an uncrowded intersection, then the VoI is identified at I_p . Let t_p denote its departure time from I_p . Then, the earliest time instant when the VoI can arrive at I_x is $t_x^s = t_p + t_{p,x}^l$. Correspondingly, $t_x^u = t_p + t_{p,x}^u$ is the latest time instant when the VoI can arrive at I_x . Thus, the latest time instant when the VoI departs from I_x is $t_x^e = t_x^u + t_x^u$, which is the time instant when the last video frame captured from I_x may contain the VoI. Thus, the edge node needs D_x time units to process the last frame and the edge node ends up processing video frames at $t_x^e = t_x^u + t_x^u + D_x$.
- **Case 2:** If the previous intersection I_p is a crowded intersection and we assume that the active period of the edge node at I_p is $[t_p^s, t_p^e]$. According to the definition of active period, the earliest time when the VoI enters I_p is no earlier than t_p^s , then the earliest time when the VoI enters I_x is no earlier than $t_x^s = t_p^s + t_{p,x}^l$; the latest time when the VoI departs from I_p is no later than $t_p^e - D_p$, then the latest time when the VoI departs from I_x is no later than $t_x^e = t_p^e - D_p + t_{p,x}^u + t_{p,x}^u$. Again, the edge node needs D_x time units to process the last frame and the edge node ends up processing video frames at $t_x^e = t_p^e - D_p + t_{p,x}^u + t_{p,x}^u + D_x$.

In light of the above discussion, the active period for the edge node at intersection I_x is calculated based on the active period of the previous edge node. Thus, we need to define the active period for the first edge node at intersection I_o where the hit-and-run accident happens. Let t_o denote the time instant when the accident is reported. Then, whether or not I_o is a crowded intersection, the active period of the edge node at I_o is $[t_o, t_o + t_o^u + D_o]$. Based on I_o 's active period, the active periods for all the involved edge nodes can be calculated one-by-one at run time.

7 WATCHDOG

In this section, we put all the proposed techniques together to build the real-time tracking system - WatchDog.

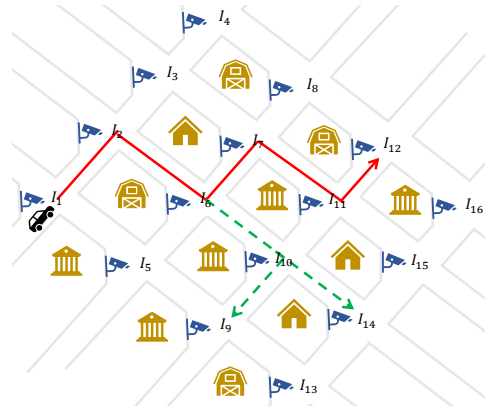


Fig. 7. An illustration example for tracking an VoI.

7.1 System Description

Fig 6 illustrates the architecture of WatchDog implemented on each edge node, which consists of four major components: (i) a live video stream generated by the surveillance camera; (ii) D-V-ReID framework; (iii) the Real-time admission control module; (iv) the Real-time Vehicle ReID program. On each edge node, each frame of the real-time video stream is firstly processed by a vehicle detection module to detect the vehicles traveling through this intersection, which is introduced in Sec. 4.1. A real-time ReID task will be performed on each detected vehicle to identify whether or not the VoI appears. Suppose the system detected n vehicles at this intersection, then the real-time task set contains n tasks. According to the D-V-ReID framework introduced in Sec. 4.2, each task has several optional execution times, which correspond to different sub-modules, which is introduced in Sec. 4.3. The longer a real-time task executes, the better ReID performance the real-time task can get. In order to guarantee that each real-time task can complete by its deadline, the real-time admission control module is performed to select the best combination of execution times for real-time tasks to ReID the VoI, according to the optimal solution for the programming, which is given by Eq. 2. Intuitively, it is a trade-off between the ReID performance and the schedulability of the real-time task system. When the modules of ReID program are chosen for each real-time task, the real-time V-ReID starts performing on each frame to track the VoI.

In light of WatchDog's architecture on each edge node, the tracking behavior of WatchDog can be described as follows:

- (1) When a hit-and-run accident is reported at time instant t_o^s from intersection I_o , WatchDog activates the first edge node deployed at I_o to track the VoI and its active period is $[t_o^s, t_o^e]$. According to the number of vehicles detected at I_o , the proper machine learning modules are selected. By performing the real-time machine learning tasks on the detected vehicles, all the suspected vehicles and the next intersections on these vehicles' trajectories are identified. If I_o is an uncrowded intersection, the VoI and the next intersection on the VoI's trajectory are identified. Then WatchDog activates all the edge nodes at the next intersections according to their active periods. Again, if I_o is an uncrowded intersection, then only one next edge node will be activated.
- (2) The edge node deployed at I_x is activated to track the VoI if the VoI or some suspected vehicles are identified at its neighboring intersection I_{x-1} and traveling to I_x . The edge node's active period is $[t_x^s, t_x^e]$, which is calculated based on the active period of the previous edge node. The calculation method is introduced in Sec. 6. Again,

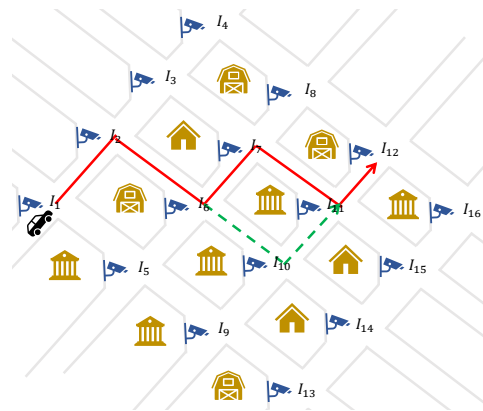


Fig. 8. The edge node at I_{11} is activated to track the VoI by multiple edge nodes deployed at neighboring intersections I_7 and I_{10} . Since the active period of an edge node is calculated based on the active period of its previous edge node, the edge node at I_{11} may have multiple active periods. If these periods overlap with each other, then the edge node's active period is a union of them.

similar to the first edge node, the proper machine learning modules are selected and performed to track all suspected vehicles traveling through this intersection during its active period.

- (3) Once the VoI is identified at any uncrowded intersection, all the suspected tracking branches are terminated.

Step 2 and Step 3 are repeated iteratively to track the VoI in real-time.

Example 3. We use a simple example to illustrate how the whole tracking system works in Fig. 7. Suppose a Mercedes silver GLB SUV is reported to be involved in a hit-and-run accident at intersection I_1 at time instant t_1^s . The edge node at I_1 is activated to track the VoI. According to the number of vehicles detected from each frame, the admission control algorithm selects the most granular algorithm for the real-time ReID tasks to track the VoI and the VoI is found to travel to I_2 . Then the edge node at I_2 is activated during to its active period. I_2 is an uncrowded intersection and the VoI is found to travel to I_6 . However, I_6 is a crowded intersection and according to the number of vehicles detected from each frame, the admission control model selects color matching module for the real-time ReID tasks to track all the silver vehicles traveling through I_6 . At I_6 , some silver vehicles are found to travel to I_7 and the others are found to travel to I_{10} . Then, the edge nodes at I_7 and I_{10} are activated to track all the silver vehicles. I_{10} is another crowded intersection and according to the number of vehicles detected from each frame, the admission control model selects color matching and model/make matching for the ReID tasks to track all suspected vehicles. Fortunately, I_7 is an uncrowded intersection and the VoI is identified at I_7 , then all the other suspected tracking branches are terminated. The following involved edge nodes are activated in the same way to track the VoI in real-time. Note that a corner case is discussed in the captain of Fig. 11.

Based on the above discussion, WatchDog can guarantee 100% tracking coverage of the VoI without “tracking loss”. We sacrifice the accuracy of ReID algorithms and track all the suspected vehicles at crowded intersections, then identify the VoI by utilizing the computing resource on the edge nodes deployed at uncrowded intersections. In a word, we develop a smart tracking method to make up for the limited computing capacity of a single edge node.

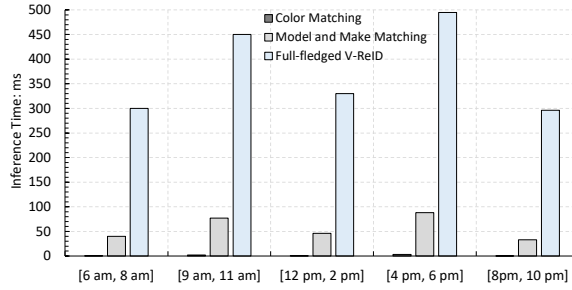


Fig. 9. The average inference time at different granularity levels.

8 EMPIRICAL STUDY

To evaluate the reliance of the proposed image processing methods in realistic scenarios, we conduct extensive experiments based on real-world datasets. We drive a vehicle (VoI) running abnormally in the road network from March 1 to March 30, 2022, then collect captured video information of all fixed video surveillance cameras at the intersections during this month. Next, we filter and select 3000 trips, each of which contains 20-30 road segments, to run our experiments.

We compare WatchDog with widely used baselines to evaluate the overall performance, which includes two categories: model selection based baselines and non-model selection based baselines.

Model selection based baselines:

- **Adadeep**[35] This method leverages a DQN based strategy to effectively select a combination of compression techniques that balance user-specified performance goals and resource constraints.
- **SkipRec-RL**[8] This work proposes an adaptive model hidden layer selection framework for deep sequential recommender system, which learns to skip inactive hidden layers on a per-user basis.
- **Greedy strategy** A greedy strategy of selecting the most fine-grained model first under the time-bound, based on some prior knowledge.

Non-model selection based baselines: On the other hand, in order to verify the effect of the adaptive model selection method, we compare our model with the traditional static fine-grained model approach. Here we utilize the last fine-grained model mentioned in Section 4.3.3 as the baseline: Full-fledged V-ReID.

Implementation Details and Ground Truths: Our proposed methods and baselines are implemented using TensorFlow 1.14 and Python 3.6 on an edge server with AMD Ryzen 7 3700x (CPU) and one NVIDIA GeForce RTX 2080 Ti (GPU). We obtained the ground truth of the VoI's trajectories through the uploaded GPS data collected by onboard devices periodically.

8.1 Experimental results

Real-time Performance at different granularity levels. In this subsection, we evaluate the reliance of the proposed object identification algorithms at different granularity levels (i.e., Color Matching, Model and Make Matching, and Full-fledged V-ReID method). The experimental results are summarized in Fig. 9, where the X-axis denotes some typical time slots of a day, and Y-axis is the average inference time of the object identification algorithms. Based on the results, we found that the inference time of the Full-fledged V-ReID method is significantly longer than the other two algorithms'

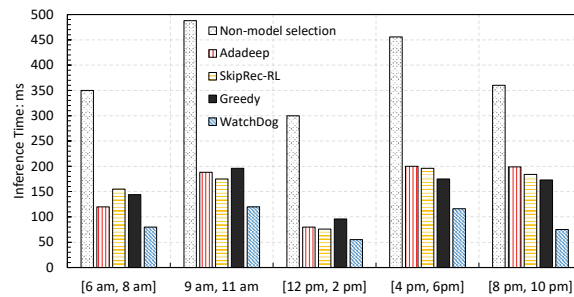


Fig. 10. The average inference time of different tracking methods.

during a day, which follows the intuition in deriving the model selection based D-V-ReID framework. In addition, the difference between them becomes larger during the rush hours (i.e., from 9 am to 11 am and from 4 pm to 6 pm). This is due to the fact that as more vehicles appear at the intersections per unit time, the Full-fledged V-ReID method will introduce more real-time workload in the embedded computing system and hence the contentions induced by the workload will exacerbate the algorithms' execution time. It suggested that during rush hours, WatchDog should start with the Color Matching module, especially at the busy intersections. Please note our evaluation is based on the real-world datasets. In our setting, a regular vehicle's Color and Make can be accurately identified. However, the plates may be blocked by some other vehicles. We have removed these imperfect data from our original datasets. In addition, we did not consider the night vision and occlusion problems in vehicle detection based on cameras due to a lack of real-world data.

Real-time Performance of different tracking methods. In this subsection, we evaluate the performance of our WatchDog solution and the Adadeep, SkipRec-RL, Greedy, Non-model selection strategies during different time periods and traffic periods, and the results are illustrated in Fig. 10. In this figure, the dark blue bar with diagonal stripes indicates the performance of our WatchDog solution, the grey bar with dotted diamond grid corresponds to the result of the non-model selection strategy, the red bar with vertical stripes gives the result of the Adadeep strategy, the orange bar with horizontal stripes represents the performance of the SkipRec-RL strategy, and the black bar indicates the performance of the Greedy strategy. And again, in Fig. 10, rush periods include 9 am - 11 am and 4 pm - 6 pm, and normal periods are equal to the rest hours. From this figure, it is clear that our WatchDog solution outperforms other alternative approaches. Moreover, we discover that the performance of our solution increases a little bit with the increase of real-time traffic compared with the other methods. This is because with the increase of road traffic, the travel speeds of the VoI decrease, thus their information is easier to be captured by our system even if the number of vehicles showing at each intersection increases. Note that in Fig. 10, the performance of the non-model selection method during 9 am - 11 am is obviously poor, the reason is that during this period the number of vehicles showing at each intersection achieves its peak value, most plates cannot be identified in real-time due to a lack of computing resources on-board, thus the information of VoIs is difficult to be obtained by the tracking system.

9 TRACE-DRIVEN EVALUATION

In addition to the empirical study, to evaluate the efficacy of WatchDog in a larger scale, we conducted extensive experiments based on our accessible real-world GPS datasets.

Table 3. Statistics of Vehicle Network

Dataset Summary	
Collection Period	6 Months
Collection Date	01/01/12-06/30/12
Number of Vehicles	14,453
Total Live Mile	371,269,642 miles

Table 4. A GPS record.

plate ID	longitude	latitude	time	speed
TIDXXXX	114.022901	22.532104	08:34:43	22 km/h

9.1 Data Description and Time/Traffic Measurement

Table 3 summarizes statistics about vehicle networks studied in this work. To test WatchDog in a real-world scenario, we utilize a real-world dataset of about 6 months of GPS traces of more than 14000 vehicles in Shenzhen, a Chinese city with a 10 million population. The dataset is obtained by letting every vehicle upload its GPS records (the format as in Table 4) to report its traces to a base station. Based on the dataset of GPS records, we obtain location and time distributions of the vehicles traveling in Shenzhen, which are used to evaluate the performance of WatchDog.

9.1.1 Measurement of traveling time. The GPS data is used to measure the traveling time of the VoI at specific locations in the monitored areas, including intersections and road segments. Fig. 5.(a) shows an example of traveling time taken by vehicles at an intersection. We can see that most of the vehicles take 5 seconds or 40 seconds to travel through this intersection. The reason is that if the traffic light at this intersection is red, the traveling time of a vehicle should include the waiting time. Due to different traveling speeds, the shortest time to travel through this intersection is 3 seconds and the longest time is 42 seconds according to Fig. 5.(a). Thus, we assume that the traveling time taken by the VoI at this intersection falls into this time interval, which is from 3 seconds to 42 seconds. Similarly, according to Fig. 5.(b), the traveling time taken by the VoI at the road segment belongs to a time interval, which is from 30 seconds to 50 seconds. By analyzing the GPS dataset, we can obtain the traveling time for the VoI at all intersections and road segments.

9.1.2 Measurement of traffic condition. Based on the time and location information in each GPS record, the datasets can be used to measure the traffic conditions in the monitored area. Figure 11 plots the percentage of the number of vehicles traveling through different intersections in one frame/one minute. At almost 16% of the intersections, only nine vehicles appear in one minute. And for more than 95% of the intersections, less than 21 vehicles travel through these intersections in one minute. These observations show that at most of the intersections, the traffic is light and our proposed method can fully utilize the edge nodes deployed at the uncrowded intersections to track the VoI in real-time.

9.2 Real-time Performance

The key performance metric for WatchDog is the video analytics delay to track the VoI in real-time. We evaluate this metric every one hour time window of a day. In addition, we investigate the sensitivities of WatchDog’s performance on three key parameters, i.e., the tracking delay, the number of involved edged nodes, as well as the tracking cost.

In order to show the impacts of different traffic conditions on WatchDog, we evaluate the performance in three typical areas in Shenzhen: Residential area, Industrial area and Commercial area, which are denoted by “Residential”, “Industrial”

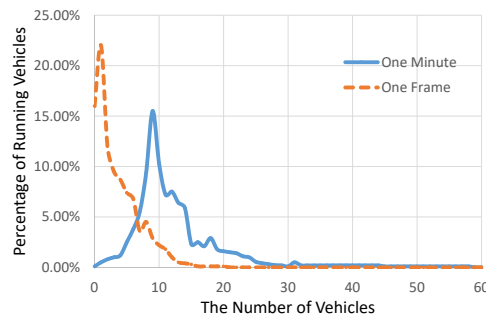


Fig. 11. The statistics of the number of vehicles traveling through an intersection in one minute/appearing on one video frame.

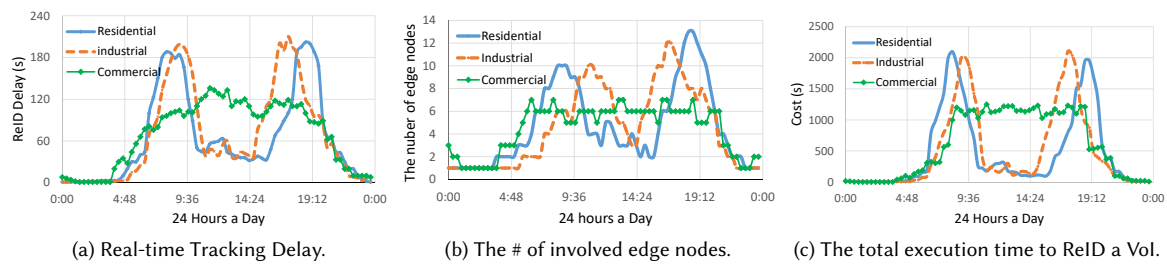


Fig. 12. The performance of Real-time tracking.

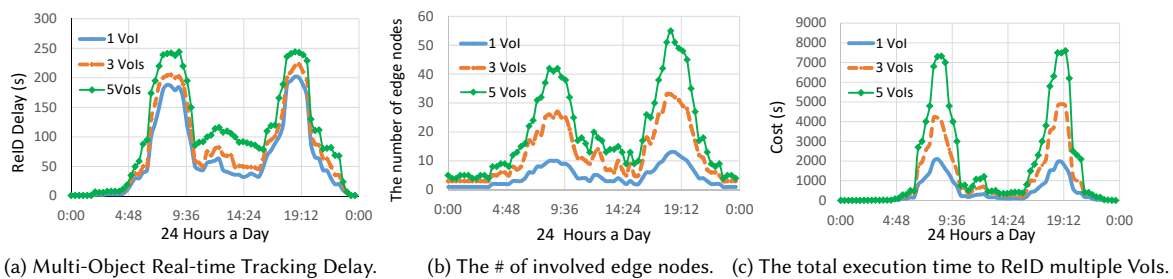


Fig. 13. The performance of Multi-Object Real-time tracking.

and “Commercial” in Fig. 12, respectively. For each tracking experiment, we randomly choose a running vehicle from the dataset as the VoI and measure the tracking delay and tracking cost according to its driving circumstance at different intersections on its trajectory according to the GPS records. The ReID modules are selected by each involved edge node automatically, based on the real-time admission control module and the number of vehicles at the intersection. The execution time for each ReID module is given in Table 2.

Fig. 12a plots the average ReID delay during 24 hours of a day. During the rush hour, e.g., 06 : 00-10 : 00, the ReID delay in three different areas reaches the maximal values. The reason is that the number of vehicles traveling through each intersection achieves the maximal value during the rush hour through the whole day. An interesting observation is that the peak of the Residential curve is earlier than the peak of the Industrial curve in the morning rush hour and on

989 the contrary in the evening. This is because the traffic flows from the residential area to industrial area in the morning
990 and reversely in the evening. As seen in this figure, even during the rush hour, the ReID delay is smaller than 4 minutes,
991 confirming that WatchDog can track the VoI in real-time.
992

993 Fig. 12b plots the average number of edge nodes involved in tracking a VoI during 24 hours of a day. As seen in this
994 figure, the maximum number of edge nodes involved in tracking a VoI is smaller than 14 even during the rush hour.
995 This implies that through carefully selecting ReID modules for the edge nodes, WatchDog is able to efficiently reduce
996 the number of suspected VoIs and limit the tracking range into a reasonably small area. Moreover, compared with the
997 residential area and industrial area, the number of involved edge nodes to track a VoI in commercial area in the rush
998 hour is much smaller. This is because the workplaces for residents are distributed in the industrial area, thus the traffic
999 in the commercial area is not as heavy as that in residential/industrial areas during the rush hours.
1000

1001 We have also conducted a set of experiments evaluating the tracking cost in the three areas in terms of the total
1002 tracking time of all involved edge nodes to ReID a VoI 24 hours a day. This metric can also be used to reflect the
1003 effectiveness of WatchDog since a shorter total tracking time to ReID and localize a VoI often results in a lower execution
1004 cost for the whole tracking system. Fig. 12c shows the result using this metric. As seen, WatchDog can track the VoI
1005 with very few edge resources during non-rush hours and the cost for real-time tracking during the rush hour is also
1006 reasonable.
1007
1008

1009 9.3 Multi-Object Tracking

1010 In this set of experiments, we evaluate the efficacy of WatchDog when handling the practical issue of multi-object
1011 real-time tracking (i.e., multiple hit-and-run accidents occur at the same time). Fig. 13 shows the evaluation results. We
1012 randomly choose multiple running vehicles (i.e., 3 and 5) as the VoIs and track them simultaneously according to the
1013 GPS datasets. We use the metric “ReID delay” (in seconds) to reflect the tracking latency of WatchDog. Similarly, we
1014 use the metrics, “the number of involved edge nodes” and “Cost”, to show the total execution time of the edge nodes
1015 consumed by WatchDog when tracking the multiple VoIs in real-time.
1016
1017

1018 Fig. 13 shows the results w.r.t. the multi-object real-time tracking. As seen in the figure, with increased number
1019 of VoIs, all the measured parameters increase during all time intervals. This observation confirms the intuition that
1020 as more VoIs are involved in real-time tracking, a larger amount of edge resources is needed to track all the VoIs
1021 simultaneously. One interesting observation is that the amount of increased edge resources is not proportional to the
1022 number of increased VoIs. For example, in Fig. 13c, the cost for tracking 1 VoI achieves its maximum value at around
1023 8:00 AM, which is about 2000 seconds. However, the cost for tracking 5 VoIs at 8:00 AM is less than 8000 seconds.
1024 This implies that the intersections involved in tracking the 5 VoIs have overlaps with each other and the video frame
1025 processing results are reused to track different VoIs. Another observation in Fig. 13a is that the ReID Delays for tracking
1026 different number of VoIs are very close. The reason is that our proposed WatchDog is a distributed real-time tracking
1027 system, which can perform the multi-object tracking simultaneously.
1028
1029

1030 10 CONCLUSION

1031 Recent technology advances in edge computing provide new opportunities to implement a real-time tracking system in
1032 smart cities with edge nodes distributed at the intersections of the road network, which consists of both surveillance
1033 cameras and embedded computing platforms. We propose a simple yet effective real-time system for tracking hit-and-run
1034 vehicles in smart cities, which employs machine learning tasks with different resource-accuracy trade-offs, and schedule
1035 tracking tasks across distributed edge nodes based on the number of detected vehicles to maximize the execution time
1036
1037
1038
1039

of tasks while ensuring a provable completion time-bound at each edge node. WatchDog is also designed to be capable of addressing multi-object tracking problems to track multiple VoIs simultaneously in real-time.

REFERENCES

- [1] [n.d.]. *Microsoft Azure Stack Edge*. <https://azure.microsoft.com>.
- [2] Geiger Andreas, Lenz Philip, and Urtasun Raquel. 2012. Are we ready for Autonomous Driving? The KITTI Vision Benchmark Suite. In *CVPR*. IEEE.
- [3] Erhan Bas, A Murat Tekalp, and F Sibel Salman. 2007. Automatic vehicle counting from video for traffic flow analysis. In *2007 IEEE intelligent vehicles symposium*. Ieee, 392–397.
- [4] Karsten Behrendt. [n.d.]. Boxy Vehicle Detection in Large Images. In *ICCV 2019*.
- [5] He Bing, Li Jia, Zhao Yifan, and Tian Yonghong. [n.d.]. Part-regularized Near-duplicate Vehicle Re-identification. In *CVPR 2019*.
- [6] Michael Bramberger, Josef Brunner, Bernhard Rinner, and Helmut Schwabach. [n.d.]. Real-time video analysis on an embedded smart camera for traffic surveillance. In *RTAS 2004*.
- [7] Xianbin Cao, Changxia Wu, Jinhe Lan, Pingkun Yan, and Xuelong Li. 2011. Vehicle detection and motion analysis in low-altitude airborne video under urban environment. *IEEE Transactions on Circuits and Systems for Video Technology* 21, 10 (2011), 1522–1533.
- [8] Lei Chen, Fajie Yuan, Jiayi Yang, Xiang Ao, Chengming Li, and Min Yang. 2021. A User-Adaptive Layer Selection Framework for Very Deep Sequential Recommender Models. In *Proceedings of the AAAI Conference on Artificial Intelligence*, Vol. 35. 3984–3991.
- [9] Opitz David and Maclin Richard. [n.d.]. Popular Ensemble Methods: An Empirical Study. *JAIR* 1999 ([n.d.]).
- [10] Zheng Dong, Linghe Kong, Peng Cheng, Liang He, Yu Gu, Lu Fang, Ting Zhu, and Cong Liu. 2014. REPC: Reliable and efficient participatory computing for mobile devices. In *2014 Eleventh Annual IEEE International Conference on Sensing, Communication, and Networking (SECON)*. IEEE, 257–265.
- [11] Zheng Dong, Cong Liu, Soroush Bateni, Zelun Kong, Liang He, Lingming Zhang, Ravi Prakash, and Yuqun Zhang. 2018. A General Analysis Framework for Soft Real-Time Tasks. *IEEE Transactions on Parallel and Distributed Systems* 30, 6 (2018), 1222–1237.
- [12] Guru DS, Y.H. Sharath, and S. Manjunath. [n.d.]. Texture Features and KNN in Classification of Flower Images. *IJCA 2010* ([n.d.]).
- [13] Tafazzoli Faezeh, Frigui Hichem, and Nishiyama Keishin. [n.d.]. A large and diverse dataset for improved vehicle make and model recognition. In *CVPR 2017*.
- [14] Rajamanoharan Georgia, Kanaci Aytac, Li Minxian, and Gong Shaogang. [n.d.]. Multi-Task Mutual Learning for Vehicle Re-Identification. In *CVPR 2019*.
- [15] Ross Girshick. [n.d.]. Fast R-CNN. In *ICCV 2015*.
- [16] Rafael C Gonzales and Richard E Woods. 2002. Digital image processing.
- [17] Hector Gonzalez, Jiawei Han, Xiaolei Li, Margaret Myslinska, and John Paul Sondag. 2007. Adaptive fastest path computation on a road network: a traffic mining approach. In *33rd International Conference on Very Large Data Bases, VLDB 2007*. Association for Computing Machinery, Inc, 794–805.
- [18] Wang Guanshuo, Yuan Yufeng, Chen Xiong, Li Jiwei, and Zhou Xi. [n.d.]. Learning Discriminative Features with Multiple Granularities for Person Re-Identification. In *MM 2018*.
- [19] Kaiming He, Xiangyu Zhang, Shaoqing Ren, and Jian Sun. [n.d.]. Deep residual learning for image recognition. In *CVPR 2016*.
- [20] Bay Herbert, Ess Andreas, Tuytelaars Timne, and Van Gool Luc. [n.d.]. Speeded-up robust features (SURF). *CVIU 2008* ([n.d.]).
- [21] Chien-Chun Hung, Ganesh Ananthanarayanan, Peter Bodik, Leana Golubchik, Minlan Yu, Victor Bahl, and Matthai Philipose. 2018. VideoEdge: Processing Camera Streams using Hierarchical Clusters. In *ACM/IEEE SEC*.
- [22] Hsu Hung-Min, Huang Sung-Wei, Wang Gaoang, Cai Jiarui, Lei Zhichao, and Hwang Jenq-Neng. [n.d.]. Multi-camera Tracking of Vehicles based on Deep Features Re-ID and Trajectory-based Camera Link Models. In *CVPR 2019*.
- [23] Yusuke Ishii. 2005. Monitor system for monitoring suspicious object. US Patent App. 11/150,264.
- [24] Spanhel Jakob, Bartl Vojtech, and Herout Adam. [n.d.]. Vehicle Re-identification and Multi-camera Tracking in Challenging City-scale Environment. In *CVPR 2019*.
- [25] Junchen Jiang, Yuhao Zhou, Ganesh Ananthanarayanan, Yuanchao Shu, and Andrew A. Chien. [n.d.]. Networked Cameras Are the New Big Data Clusters. In *Hot edge 2019*.
- [26] Hu Jie, Shen Li, and Sun Gang. 2018. Squeeze-and-Excitation Networks. *IEEE Conference on Computer Vision and Pattern Recognition (CVPR)*.
- [27] Dai Jifeng, Li Yi, He Kaiming, and Sun Jian. [n.d.]. R-FCN: Object Detection via Region-based Fully Convolutional Networks. In *NIPS 2016*.
- [28] So Yeon Jo, Namhyun Ahn, Yunsoo Lee, and Suk-Ju Kang. [n.d.]. Transfer Learning-based Vehicle Classification. In *ISOCC 2018*.
- [29] Redmon Joseph and Farhadi Ali. 2018. YOLOv3: An Incremental Improvement. *arXiv preprint arXiv:1804.02767* (2018).
- [30] Redmon Joseph, Divvala Santosh, Girshick Ross, and Farhadi Ali. [n.d.]. You Only Look Once: Unified, Real-Time Object Detection. In *CVPR 2016*.
- [31] He Kaiming, Georgia, and Dollár Piotr. [n.d.]. Mask R-CNN. In *ICCV 2017*.
- [32] Guillaume Leduc et al. [n.d.]. Road traffic data: Collection methods and applications. *Working Papers on Energy, Transport and Climate Change 2008* ([n.d.]).
- [33] Hennadiy Leontyev and James H Anderson. [n.d.]. Tardiness bounds for FIFO scheduling on multiprocessors. In *ECRTS'07*.

- 1093 [34] Honghai Liu, Shengyong Chen, and Naoyuki Kubota. 2013. Intelligent video systems and analytics: A survey. *IEEE Transactions on Industrial*
1094 *Informatics* 9, 3 (2013), 1222–1233.
- 1095 [35] Sicong Liu, Yingyan Lin, Zimu Zhou, Kaiming Nan, Hui Liu, and Junzhao Du. 2018. On-demand deep model compression for mobile devices: A
1096 usage-driven model selection framework. In *Proceedings of the 16th Annual International Conference on Mobile Systems, Applications, and Services*.
1097 389–400.
- 1098 [36] Yin Lou, Chengyang Zhang, Yu Zheng, Xing Xie, Wei Wang, and Yan Huang. 2009. Map-matching for low-sampling-rate GPS trajectories. In
1099 *Proceedings of the 17th ACM SIGSPATIAL international conference on advances in geographic information systems*. 352–361.
- 1100 [37] David G. Lowe. [n.d.]. Object Recognition from Local Scale-Invariant Features. In *ICCV 1999*.
- 1101 [38] Rongxing Lu, Xiaodong Lin, Haojin Zhu, and Xuemin Shen. 2009. SPARK: A new VANET-based smart parking scheme for large parking lots. In
1102 *IEEE INFOCOM 2009*. IEEE, 1413–1421.
- 1103 [39] Cordts Marius, Omran Mohamed, Ramos Sebastian, Rehfeld Timo, Enzweiler Markus, Benenson Rodrigo, Franke Uwe, Roth Stefan, and Schiele
1104 Bernt. [n.d.]. Feature Pyramid Networks for Object Detection. In *CVPR 2016*.
- 1105 [40] Dalal Navneet and Triggs Bill. [n.d.]. Histograms of oriented gradients for human detection. In *CVPR 2005*.
- 1106 [41] Boonsim Noppakun and Prakoonwit Simant. [n.d.]. Car make and model recognition under limited lighting conditions at night. *CVIU 2017* ([n. d.]).
- 1107 [42] Khorramshahi Pirazh, Kumar Amit, Peri Neehar, Sai Saketh Rambhatla, Chen Jun-Cheng, and Chellappa Rama. [n.d.]. A Dual-Path Model With
1108 Adaptive Attention For Vehicle Re-Identification. In *ICCV 2019*.
- 1109 [43] Khorramshahi Pirazh, Peri Neehar, Kumar Amit, Shah Anshul, and Chellappa Rama. [n.d.]. Attention Driven Vehicle Re-identification and
1110 Unsupervised Anomaly Detection for Traffic Understanding. In *CVPR 2019*.
- 1111 [44] Baran Remigiusz, Glowacz Andrzej, and Matiolanski Andrzej. [n.d.]. The efficient real- and non-real-time make and model recognition of cars. *MTA*
1112 *2015* ([n. d.]).
- 1113 [45] Mark Sandler, Andrew Howard, Menglong Zhu, Andrey Zhmoginov, and Liang-Chieh Chen. [n.d.]. MobileNetV2: Inverted Residuals and Linear
1114 Bottlenecks. In *CVPR 2018*.
- 1115 [46] E Schmitt and Hossein Jula. 2006. Vehicle route guidance systems: Classification and comparison. In *2006 IEEE Intelligent Transportation Systems*
1116 *Conference*. IEEE, 242–247.
- 1117 [47] Ren Shaoqing, He Kaiming, Girshick Ross, and Sun Jian. [n.d.]. Faster R-CNN: Towards Real-Time Object Detection with Region Proposal Networks.
1118 In *NIPS 2015*.
- 1119 [48] Kazufumi Suzuki and Hideki Nakamura. 2006. TrafficAnalyzer-the integrated video image processing system for traffic flow analysis. In *Proceedings*
1120 *of the 13th ITS World Congress, London, 8-12 October 2006*.
- 1121 [49] Mingxing Tan and Quoc V. Le. [n.d.]. EfficientNet: Rethinking Model Scaling for Convolutional Neural Networks. In *ICML 2019*.
- 1122 [50] Huang Tsung-Wei, Cai Jiarui, Yang Hao, Hsu Hung-Min, and Hwang Jenq-Neng. [n.d.]. Multi-view Vehicle Re-identification Using Temporal
1123 Attention Model and Metadata Re-ranking. In *CVPR 2019*.
- 1124 [51] Lin Tsung-Yi, Goyal Priya, Girshick Ross, He Kaiming, and Dollár Piotr. [n.d.]. Focal Loss for Dense Object Detection. In *ICCV 2017*.
- 1125 [52] V.F.Rodriguez-Galiano, B.Ghimire, J.Rogan, M.Chica-Olmo, and J.P.Rigol-Sanchez. [n.d.]. An assessment of the effectiveness of a random forest
1126 classifier for land-cover classification. *ISPRS 2012* ([n. d.]).
- 1127 [53] Fei-Yue Wang. 2010. Parallel control and management for intelligent transportation systems: Concepts, architectures, and applications. *IEEE*
1128 *Transactions on Intelligent Transportation Systems* 11, 3 (2010), 630–638.
- 1129 [54] Yang Wang, Wuji Chen, Wei Zheng, He Huang, Wen Zhang, and Hengchang Liu. 2017. Tracking hit-and-run vehicle with sparse video surveillance
1130 cameras and mobile taxicabs. In *2017 IEEE International Conference on Data Mining (ICDM)*. IEEE, 495–504.
- 1131 [55] Liu Wei, Anguelov Dragomir, Erhan Dumitru, Szegedy Christian, Reed Scott, Fu Cheng-Yang, and C. Berg Alexander. 2016. SSD: Single Shot
1132 MultiBox Detector. In *European Conference on Computer Vision (ECCV)*. Springer.
- 1133 [56] Chen Weihua, Chen Xiaotang, Zhang Jianguo, and Huang Kaiqi. [n.d.]. A Multi-task Deep Network for Person Re-identification. In *AAAI 2017*.
- 1134 [57] Tan Xiao, Wang Zhigang, Jiang Minyue, Yang Xipeng, Wang Jian, Gao Yuan, Su Xiangbo, Ye Xiaoqing, Yuan Yuchen, He Dongliang, Wen Shilei, and
1135 Ding Errui. [n.d.]. Multi-camera Vehicle Tracking and Re-identification Based on Visual and Spatial-temporal Features. In *CVPR 2019*.
- 1136 [58] Zhang Yu, Wei Ying, and Yang Qiang. 2018. Learning to Multitask. In *NeurIPS*.
- 1137 [59] Junping Zhang, Fei-Yue Wang, Kunfeng Wang, Wei-Hua Lin, Xin Xu, and Cheng Chen. 2011. Data-driven intelligent transportation systems: A
1138 survey. *IEEE Transactions on Intelligent Transportation Systems* 12, 4 (2011), 1624–1639.
- 1139 [60] Xiangyu Zhang, Xinyu Zhou, and Jian Sun. [n.d.]. ShuffleNet: An Extremely Efficient Convolutional Neural Network for Mobile Devices. In *CVPR*
1140 *2018*.
- 1141 [61] Wang Zhongdao, Tang Luming, Liu Xihui, Yao Zhuliang, Yi Shuai, and Jing. [n.d.]. Orientation invariant feature embedding and spatial temporal
1142 regularization for vehicle reidentification. In *ICCV 2017*.